

Impact of LVRT Capability of Wind Turbines on Distance Protection of AC Grids

Lina He, *Student Member, IEEE*, Chen-Ching Liu, *Fellow, IEEE*,

Abstract— When a transmission line close to a wind farm (WF) with doubly fed induction generators (DFIGs) experiences a short circuit (SC) fault, the resulting voltage dip on the WF terminal bus may trigger actions from the crowbar circuits of DFIGs. These actions prevent high rotor currents that can be damaging to power electronic converters. Under this condition, DFIGs have to absorb reactive power from the external power grid to provide generator excitation. As a result, it will further depress the voltage at the WF terminal bus and affect the protective relay operation of transmission lines in severe situations. This paper is concerned with the performance of distance relays on a power grid with WFs that are equipped with crowbar circuits. Numerical simulations are conducted on IEEE 39 bus system with WF connections. It is found that the fault on the terminal line of a WF is likely to induce mis-coordination of distance relays, leading to system security problems.

Index Terms— WFs, DFIGs, low voltage ride through (LVRT), crowbar circuits, distance relays, protection mis-coordination.

I. INTRODUCTION

WITH the increasing energy demand and growing environmental concern, the integration of renewable energy sources, e.g., wind power, has been significantly increased [1]. Currently, the technologies of wind power generation can be divided into two basic categories: fixed and variable speed. The fixed-speed wind turbine technology applies the conventional squirrel cage induction generator to convert mechanical power from the wind turbine into electrical power. Its normal operation needs to absorb reactive power from the external grids to provide generator excitation. It has been shown that the behavior can further depress the terminal voltage during voltage dips [2]. As a result, reactive power compensation devices, such as capacitors or STATCOM, are installed with fixed-speed wind generators to compensate for the reactive power demand.

With the innovation of wind technologies, the variable-speed wind turbine technology has demonstrated to overcome the limitations of fixed speed wind generators [3]. Variable-speed wind generators allow variable rotor speed that helps to improve the efficiency by capturing power over a wider range of wind speed. In addition, the variable-speed wind turbine technology enables the regulation of power factor by

absorbing or producing reactive power [4]. Medium and large WFs (more than 50MW) based on variable-speed wind generators have been integrated into the power grids at the transmission level. Over the last decade, the DFIG has become the dominant technology in the growing global market for wind generators. It is comprised of a wound-rotor induction generator and a power electronic dc link that connects the rotor winding and grid.

The operation of DFIGs is sensitive to terminal voltage dips. It can rapidly demagnetize the DFIG stator, leading to large outrush currents in both stator and rotor windings [2]. The outrush currents are usually higher than the ratings of power electronic converters. As a result, new grid codes for integration of wind generators require LVRT capability to maintain WF connections during voltage dips [5]. The most common way is to use a crowbar circuit. It is automatically activated to deenergize the rotor and disconnect the converter device from the rotor in case rotor windings experience high currents during a voltage dip. The action leads to the loss of DFIG controllability, allowing the DFIG to behave as a conventional squirrel cage induction generator. The generator has to absorb reactive power from the external power grid. Hence, it further deteriorates the DFIG terminal voltage.

When a transmission line close to a large wind farm with DFIGs experiences a short circuit fault, the high-slip reactive power demand of DFIGs during the crowbar connection is significant. It dramatically affects nodal voltages and line currents close to the WF. This is likely to disturb the normal operation of existing protection relays on the power grid, e.g., distance relays that are widely employed on transmission lines. The basic principle of distance relays is to measure the apparent impedance using the voltage and current viewed by a relay, which approximately determines the distance between the relay location and fault point during a SC fault [6]. The apparent impedance is then compared with pre-set relay operational characteristics to determine whether the fault is within the protected zone.

With the growing penetration of wind power, the caused impact on the performance of distance relays by reactive power absorption of DFIGs during the crowbar connection can be significant, especially for high-capacity WFs. During a SC fault, apparent impedances viewed by distance relays may not correctly indicate the actual fault location. Furthermore, it may cause mis-coordinated operations of distance relays. In a severe case, it is likely to endanger system security, leading to cascading events.

Studies have been conducted on the effect of reactive

Lina He is with University College Dublin, Belfield, Dublin 4, Ireland (e-mail: lina.he@ucdconnect.ie).

Chen-Ching Liu is with Washington State University, Pullman, WA99164-2752, USA, and University College Dublin, Belfield, Dublin 4, Ireland (e-mail: liu@ucd.ie).

power control on the performance of distance relays on transmission lines [7-9]. They mainly focus on flexible alternating current transmission system (FACTS) devices. It is found that a high level of reactive power absorption or production during faults can significantly affect the performance of distance relays and even induce relay mis-coordination. The work of [10] analyzes the performance of distance relays on a transmission line connected to a WF under different wind conditions. It also reports the identification of adaptive distance relay settings for variable wind power output. To the best of the authors' knowledge, existing research has not considered the impact of WF LVRT capability on the performance of distance relays. Therefore, it is important to identify the performance of distance relays on a power grid with WF connections during the crowbar activation and address issues of relay mis-coordination.

The organization of this paper is as follows. Section II outlines the LVRT scheme of a DFIG. Section III analyzes the impedances viewed by distance relays on the WF terminal line in case of a three-phase SC fault close to a WF. Numerical simulations are conducted on IEEE 39 bus system with and without WF connections for the performance analysis of distance relays. Simulation results are provided in Section IV. Section V gives the conclusion.

II. DFIG CROWBAR AND REACTIVE POWER PERFORMANCE

Fig. 1 shows the configuration of a DFIG with a wind turbine. The rotor windings are fed through a back-to-back power electronic dc link. It enables variable speed operation of the wind turbine and provides independent control of active and reactive power output. Converters are typically rated at about 20%-35% of the stator power [11]. It offers considerable cost savings and lower losses than a directly full-power-rated converter topology.

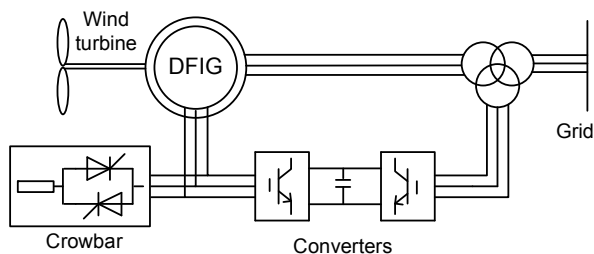


Fig. 1 Typical configuration of DFIG with wind turbine

A DFIG is generally equipped with an overcurrent crowbar and overvoltage protection in order to protect power electronic converters and avoid undesirable disconnection of the DFIG. The crowbar circuit utilizes power electronic full-controlled switches and their “turn-on” time is in the order of microsecond. It helps to rapidly divert high current from the rotor side converter and deenergize the rotor during system voltage dips. The size of the crowbar resistance determines the decay timescale of the rotor flux. A higher resistance can help accelerate the decay process, but it reduces the performance of active power. To fully deenergize the rotor, the connection duration of a crowbar is extended to maintain the DFIG

connection during faults. In actual power grids, it is typically set to 100-120ms that enables the operation of primary protection [2]. During the connection period, the DFIG operates as a conventional induction generator with a high rotor resistance. It needs to absorb high-slip reactive power to maintain the generator operation.

In new grid codes, large wind farms are required to enable system support for improving stability and reliability of transmission grids during disturbances. When the crowbar circuits of DFIGs in a WF are activated during a voltage dip, reactive power absorption of DFIGs leads to the depression of the WF terminal voltage that makes against system voltage restoration. It is reported in recent studies that the DFIG grid side converter can operate as a STATCOM during the crowbar connection to provide reactive power support for the power grid [4]. To some extent, it will help to relieve the reactive power demand of DFIGs during the crowbar connection.

According to the work of [12], the reactive power capability of a voltage source converter depends on its capacity limitation and the ac side voltage. When a converter operates at the rated ac side voltage, the maximum reactive power output is almost half of the active power capability. It can be further reduced in case the converter ac side encounters a voltage dip. Since the converter capacity is only 20%-35% of the DFIG stator power, reactive power that can be provided by the partial rated converter is limited, especially during a severe voltage dip close to a DFIG connection. Therefore, the potential benefit from the grid side converter is not sufficient to counteract high reactive power demand from the DFIG during the crowbar connection. The additional impact brought by the LVRT capability of WFs involves the abnormal operation of distance relays.

III. EFFECT OF REACTIVE POWER DEMAND OF DFIG DURING CROWBAR CONNECTION ON DISTANCE RELAY

A. Distance Protection of AC Grid

Large wind farms are being integrated into transmission levels of power grids due to their increasing capacity. As a widely adopted practice for transmission line protection, distance relaying is designed with primary and backup protection. Its operational characteristics are predefined with fixed settings based on detailed offline studies. Distance relays are arranged to provide two or three protective zones for transmission lines. Zone 1 is the primary protection that is set to protect 80%-85% of the line length and operate without an intentional time delay. As a backup, Zone 2 is required to protect the entire protected line and reach 40-50% of the shortest adjacent line with an appropriate time delay (typically 15-30 cycles) [13]. Zone 3 works as a further backup of an adjacent line in case of an unexpected failure of Zone 2 backup protection. It is generally set to overreach adjacent lines with a typical time delay of 1 s.

Fixed time delays help to coordinate different zones of distance relays. When the impedance viewed by a relay stays within the range of its protection zone for the required time delay, the relay is activated to send a tripping signal to the corresponding circuit breaker. Generally, a circuit breaker

needs 3-5 cycles to complete the opening process. The duration is called the break time, which is the time interval between energizing the trip circuit and when the arc is extinguished in all poles.

B. Discussion of Performance of Distance Relays during Crowbar Connection

Fig. 2 shows a portion of an ac grid with the connection of a WF based on DFIGs that is used for performance analysis of distance relays during the crowbar connection. Transmission lines of the ac grid are protected by distance relays: Zone 1 reaches 80% of the protected line and Zone 2 reaches up to 50% of the shortest line emanating from the remote bus with the time delay of 24 cycles (i.e., 0.4 s for 60 Hz grids). As shown in Fig. 2, a three-phase SC fault F is located on the WF terminal line j-k. It is in the range of Zone 2 of relay B and Zone 3 of relay A. Fault F is expected to be cleared by circuit breaker B with a Zone 2 time delay.

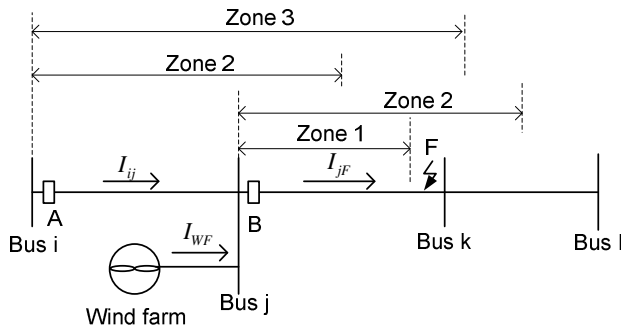


Fig. 2 Portion of power grid with WF connection

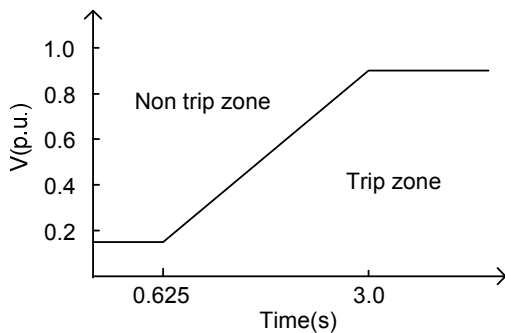


Fig. 3 LVRT voltage-duration profile in FERC order 661

When a SC fault at F is initiated, bus j encounters a voltage dip. Suppose that the voltage dip meets the ride-through requirements of the WF. The crowbar circuits of DFIGs are activated to limit the high currents of rotor windings. According to the LVRT capability standard of WF connections published by FERC in 2005, i.e. FERC Order 661, the WF connection has to be maintained for 0.625 s when its terminal voltage is higher than 0.15 p.u. [14]. The LVRT voltage-time profile of FERC Order 661 is shown in Fig. 3. It is seen that the required WF connection duration is higher than the clearing time of a Zone 2 fault (i.e. the sum of Zone 2 time delay and the break time of a circuit breaker). During fault F, the WF connection can be remained in case bus j voltage is

not lower than 0.15 p.u.. The crowbar circuits of the WF are expected to maintain the activation state until fault F is cleared.

Assuming the fault impedance is 0, the impedance viewed by relay B corresponds to the line impedance from the fault point to the relay location (Z_{BF}). It can be represented as,

$$Z_{m_B} = \frac{V_j}{I_{jF}} = Z_{BF} \quad (1)$$

where V_j and I_{jF} are the voltage and current viewed by relay B, respectively. For fault F, relay A works as a backup and its apparent impedance is given by

$$Z_{m_A} = \frac{V_i}{I_{ij}} = \frac{V_j + Z_{ij} * I_{ij}}{I_{ij}} = \frac{V_j}{I_{ij}} + Z_{ij} \quad (2)$$

where V_i and I_{ij} are the voltage and current viewed by relay A, respectively. Applying the Kirchhoff's voltage law on Bus j, V_i can be represented as a function of V_j , as shown in (2). Z_{ij} is the impedance of line i-j, which is constant. Therefore, the impedance viewed by relay A, i.e., Z_{m_A} , is determined by V_j and I_{ij} .

During the crowbar connection, the WF needs to absorb reactive power to maintain the operation of induction generators. It depresses the voltage at the WF terminal bus j and increases the current of line i-j. As a result, the impedance viewed by relay A is reduced and the fault distance viewed by relay A is underestimated. As shown in Fig. 2, fault F is located in the range of Zone 3 of relay A. Due to reactive power absorption of the WF during the crowbar connection, the Zone 3 fault is likely to be viewed as a Zone 2 event of relay A. Relay B, as a primary protection, is expected to send a tripping signal to circuit breaker B after a Zone 2 time delay. It is possible for both relays A and B to be activated. As a result, the protection mis-coordination leads to tripping of both circuit breakers A and B. Eventually, the WF is disconnected and the resulting generation deficit may cause a system security problem.

IV. CASE STUDIES

A. Simulation Systems

Case studies are based on IEEE 39 bus system that is a 345 kV, 60 Hz conventional ac grid, including 10 synchronous generators and 34 ac transmission lines with a rating of 1.5 kA. All transmission lines in IEEE 39 bus system are protected by distance relays. Zone 2 relays reach 50% of the shortest line emanating from the remote bus with the time delay of 24 cycles (i.e. 0.4 s). Their settings are identified by fault simulations in DgSILENT PowerFactory. The procedure to determine the Zone 2 settings are listed as follows:

- (1) Initiate a three-phase SC fault at the Zone 2 reach of a distance relay at 0 s in IEEE 39 bus system;
- (2) Measure the impedance viewed by the relay at the clearing time of a Zone 2 fault;
- (3) The obtained value is set as the Zone 2 setting of the relay.

By the fault simulation method, the settings of all distance relays on IEEE 39 bus system can be predetermined. The

break time of circuit breakers is set to 4 cycles.

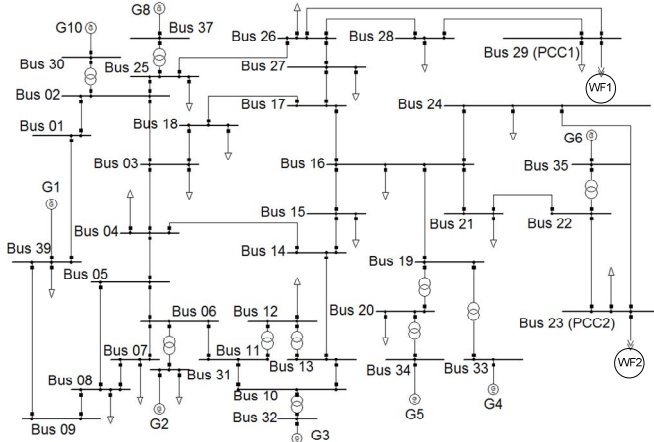


Fig. 4 IEEE 39 bus system with WF connections

As shown in Fig. 4, two WFs based on DFIGs are connected to bus 23 and 29, respectively, to replace conventional synchronous generators of IEEE 39 bus system. Wind generators are standard DFIGs each rated at 5 MW. The DFIG parameters are shown in Table III of Appendix. The LVRT protection settings of DFIGs apply the standard of FERC Order 661 and the connection duration of crowbar circuits is set to 100 ms. The scenarios of IEEE 39 bus system with WF connections are adjusted to have identical power flow results with IEEE 39 bus system. This results in an identical initial state in two systems during an identical SC fault.

Fault simulations are conducted on the IEEE 39 bus system and IEEE 39 bus system with WF connections, respectively. The performance of distance relays on two ac grids is reported in this section for the impact analysis of LVRT capability on distance relays.

B. Performance of Distance Relays in IEEE 39 Bus System

In IEEE 39 bus system, synchronous generators are connected to bus 23 and 29, respectively, as shown in Fig. 5. Line 22-23 and 23-24 are equipped with relay M and N, respectively. The settings of both relays are determined in Section IV A. A three-phase SC fault F1 located at 90% of line 23-24 is initiated at 0 s with 0 fault impedance. According to the protective zones of distance relays, fault F1 is in the range of Zone 2 of relay N and Zone 3 of relay M. During the SC fault, the impedance trajectories viewed by relays N and M are shown in Fig. 6 (a) and (b), respectively. It is noted that only circuit breaker N is tripped and its activation and tripping times are listed in Table I.

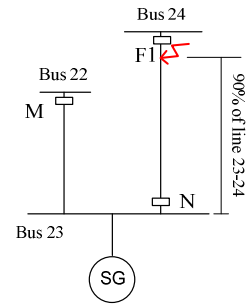
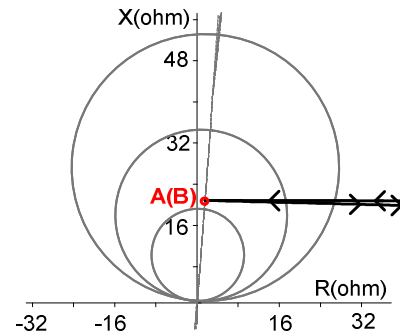
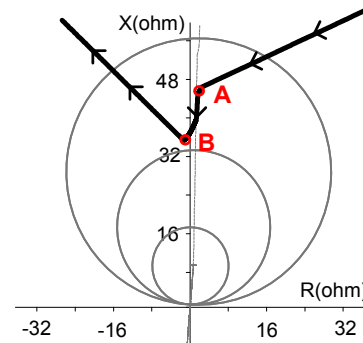


Fig. 5 Portion of IEEE 39 bus system



(a) Impedance trajectory of relay N



(b) Impedance trajectory of relay M

Fig. 6 Impedance trajectories of relays N and M in IEEE 39 bus system (A: the time of fault initiation; B: the time of circuit breaker tripping)

TABLE I

OPERATION OF CIRCUIT BREAKERS N AND N IN IEEE 39 BUS SYSTEM			
Circuit Breaker	Zone of relay operation	Activation time (sec)	Tripping time (sec)
N	Zone 2	0.40	0.47
M	-	-	-

It is shown in Fig. 6 (a) and (b) that the impedances viewed by relays N and M are, respectively, in the range of Zone 2 of relay N and Zone 3 of relay M when fault F1 is initiated. After a Zone 2 time delay, relay N is activated to send a tripping signal to circuit breaker N. After tripping of circuit breaker N, it is seen in Fig. 6 (b) that the impedance viewed by relay M falls beyond its Zone 3 range. It results in return of Zone 3 of relay M.

C. Performance of Distance Relays on IEEE 39 Bus System with WF Connections

An identical fault is located at 90% of line 23-24 in the IEEE 39 bus system with WF connections and initiated at 0 s.

The impedance trajectories viewed by relays N and M are shown in Fig. 7 (a) and (b), respectively. As shown in Table II, both circuit breakers M and N are tripped.

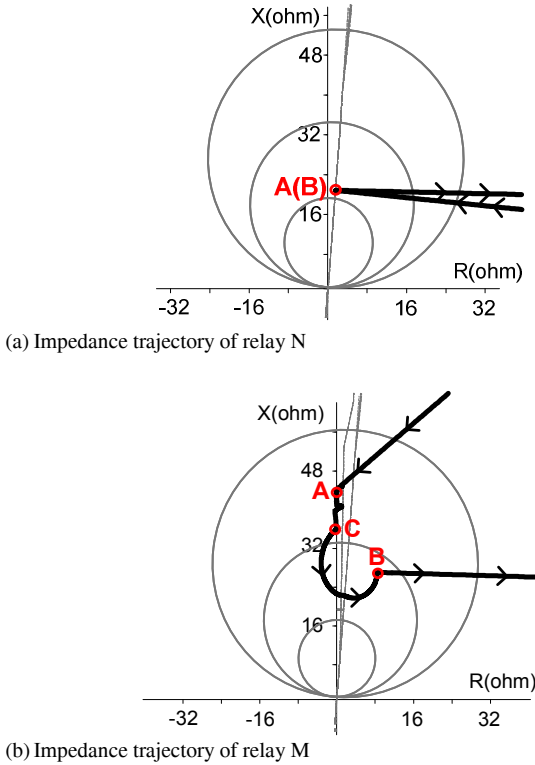


Fig. 7 Impedance trajectories of relays N and M on IEEE 39 bus system with WF connections (A: the time of fault initiation; B: the time of circuit breaker tripping)

TABLE II
OPERATION OF CIRCUIT BREAKERS N AND M IN IEEE 39 BUS SYSTEM WITH WF CONNECTIONS

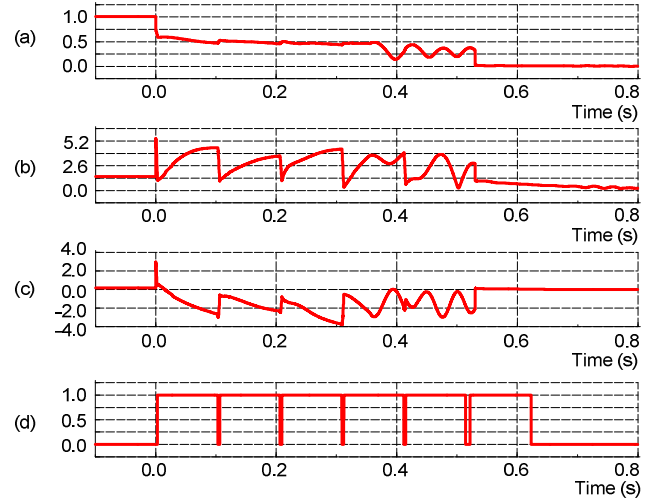
Circuit Breaker	Zone of relay operation	Activation time (sec)	Tripping time (sec)
N	Zone 2	0.40	0.47
M	Zone 2	0.44	0.51

During the fault, the impedance viewed by relay N reflects the line impedance from the fault point to the relay location for a 0 fault impedance. As the apparent impedance is a constant, the performance of relay N during the SC fault is not affected by WF additions. As shown in Table II, relay N is tripped at 0.47 s that is same as the tripping time of relay N on IEEE 39 bus system. In addition, the impedance trajectory of relay N in Fig. 7 (a) is almost identical to that in the IEEE 39 bus system.

However, the impedance trajectory in Fig. 7 (b) is different from that in Fig. 6 (b). When the fault is initiated (point A in Fig. 7 (b)), the corresponding impedance viewed by Relay M is in the range of its Zone 3. The impedance drop during the fault in Fig. 7 (b) is divided into two periods, i.e. A-C and C-B. It is seen that the trend of the impedance drop on A-C is similar to that on A-B in Fig. 6 (b). This period corresponds to the subtransient state during the SC fault.

After point C, the impedance viewed by relay M is

gradually reduced and finally reaches the range of Zone 2 at 0.04 s. As shown in Table II, relay N is activated after a Zone 2 time delay. Due to the break time of 4 cycles, circuit breaker N is tripped at 0.47 s. Before the tripping of circuit breaker N, relay M is mis-coordinated and sends a tripping signal to circuit breaker M at 0.44 s. As a result, both circuit breakers M and N are tripped.



(a) Terminal voltage of WF2 (p.u.)
(b) Rotor current of DFIG in WF2 (p.u.)
(c) Reactive power output of WF2 (p.u.)
(d) Activation signal of DFIG crowbar circuits in WF2 ('1' means activation of crowbar circuit; '0' means deactivation of crowbar circuit)

Fig. 8 Dynamics of WF2 during SC fault

During the fault, the dynamics of the WF2 are shown in Fig. 8, including the terminal voltage of WF2, the DFIG rotor current, reactive power output of WF2 and the activation signal of crowbar circuits. The system base for per unit quantities is 100 MVA. It is seen in Fig. 8 (a) that the terminal voltage of WF2 is reduced to about 0.6 p.u. when the SC fault is initiated on line 23-24. It leads to dramatic increases in the rotor currents of DFIGs, as shown in Fig. 8 (b). DFIG crowbar circuits are triggered to divert the high rotor currents from power electronic converters. It is found in Fig. 8 (d) that the activation signal of crowbar circuits is stepped to "1" from "0". During the crowbar connection, DFIGs lose controllability and operate as induction generators. They need to absorb reactive power from the ac grid to support the operation. It is found in Fig. 8 (c) that reactive power output of WF2 becomes negative at about 0.02 s. It results in further reduction of the terminal voltage of WF2 in Fig. 8 (a).

Crowbar circuits are disconnected after 100 ms due to the pre-set connection duration, as shown in Fig. 8 (d). Since the SC fault has not been cleared and the terminal voltage dip still exists, it is seen that crowbar circuits are activated again. This behavior is repeated several times until the fault is cleared. During this period, DFIGs continue absorbing reactive power from the ac grid and result in gradual reduction of the terminal bus 23 voltage. As a result, the impedance viewed by relay M is decreased and the Zone 3 fault is viewed by relay M as a Zone 2 event. Eventually, Zone 2 of both relays M and N are

activated. The resulting protection mis-coordination disconnects the WF2 from the ac grid, leading to a generation deficit.

V. CONCLUSION

When crowbar circuits of DFIGs in a WF are activated during a SC fault, DFIGs operate as conventional induction generators. They have to absorb reactive power from the external power grid to provide the stator excitation. This is likely to affect the normal operation of distance relays. A fault simulation case conducted on IEEE 39 bus system with WF connections is reported in this paper. It is concluded that reactive power absorption of DFIGs during the crowbar connection can result in protection mis-coordination of distance relays. With the growing penetration of wind farms, a sizable addition of WF connections is being connected to the transmission level of power grids. The issue of protection mis-coordination caused by LVRT capability of WFs can be significant. Under extreme conditions, it could endanger security of power grids.

Some requirements about reactive power output of DFIGs have been proposed in new grid codes. Due to the capacity limitation of power electronic converters, they are not sufficient for the reactive power demand of DFIGs in case WF terminals experience severe voltage dips. Additional reactive power devices may be beneficial for WF connections to reduce the risk of protection mis-coordination.

APPENDIX

TABLE III
PARAMETERS OF 5 MW DFIG

Parameters	Value
Stator Resistance	0.003 p.u.
Stator Reactance	0.125 p.u.
Magnetizing Reactance	2.5 p.u.
Rotor Resistance	0.004 p.u.
Rotor Reactance	0.05 p.u.
Acceleration Time Constant	0.5s

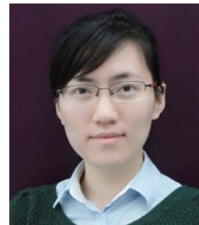
ACKNOWLEDGEMENT

The authors would like to acknowledge the support from the EU project "Twenties," Transmission system operation with large penetration of Wind and other renewable Electricity sources in Networks by means of innovative Tools and Integrated Energy Solutions.

REFERENCES

- [1] K. Bell, D. Cirio, A.M. Denis, L. He, C.-C. Liu, C. Moreira, and P. Panciatici, "Economic and technical criteria for designing future offshore HVDC grids," *IEEE PES: Innovative Smart Grid Technologies Europe 2010*.
- [2] C. Pannell, D.J. Atkinson, and B. Zahawi, "Minimum-threshold crowbar for a fault-ride-through grid-code-compliant DFIG wind turbine," *IEEE Trans. on Energy Convers.*, vol. 22, no. 3, pp. 976-984, Aug. 2007.
- [3] L. Holdsworth, X.G. Wu, J.B. Ekanayake, and N. Jenkins, "Comparison of fixed speed and doubly-fed induction generator wind turbines during power system disturbances," *IEE Proceedings-Generation, Transmission and Distribution*, vol. 150, no. 3, pp. 343-352, May. 2003

- [4] D. Xiang, L. Ran, P.J. Tavner, and S. Yang, "Control of a doubly fed induction generator in a wind turbine during grid fault ride-through," *IEEE Trans. on Energy Convers.*, vol. 21, no. 3, pp. 652-662, Sep. 2006.
- [5] J. Morren, and S.W. Haan, "Ride through of wind turbines with doubly-fed induction generator during a voltage dip," *IEEE Trans. on Energy Convers.*, vol. 20, no. 2, pp. 435-441, June 2005.
- [6] P.M. Anderson. *Power System Protection*. NewYork: The Institute of Electrical and Electronics Engineers, 1999.
- [7] T. S. Sidhu, R. K. Varma, P. K. Gangadharan, F. A. Albasri, and G. R. Ortiz, "Performance of distance relays on shunt-FACTS compensated transmission lines," *IEEE Trans. on Power Del.*, vol. 20, no. 3, pp. 1837-1845, July 2005.
- [8] X. Zhou, H. Wang, R. K. Aggarwal, and P. Beaumont, "Performance evaluation of a distance relay as applied to a transmission system with UPFC," *IEEE Trans. on Power Del.*, vol. 20, no. 3, pp. 1237-1147, July 2006.
- [9] P. K. Dash, A. K. Pradhan, G. Panda, and A. C. Liew, "Adaptive relay setting for flexible AC transmission system (FACTS)," *IEEE Trans. on Power Del.*, vol. 15, no. 1, pp. 38-43, Jan. 2000.
- [10] A. K. Pradhan and G. Joos, "Adaptive distance relay setting for lines connecting wind farms," *IEEE Trans. on Power Del.*, vol. 22, no. 1, pp. 206-213, Mar. 2007.
- [11] J. Lopez, E. Gubia, E. Olea, J. Ruiz, and L. Marroyo, "Ride through of wind turbines with doubly fed induction generator under symmetrical voltage dips," *IEEE Trans. on Ind. Electron.*, vol. 56, no. 10, pp. 4246-4254, Oct. 2009.
- [12] M. Larsson, "HVDC and HVDC light – an alternative power transmission system", *Symposium on Control & Modeling of Alternative Energy Systems*, April, 2009.
- [13] N. Acharya and C.-C. Liu, "Tripping of wind turbines during a system fault," *Proc. 2008 IEEE PES General Meeting*, pp. 1-8, 20-24, July 2008.
- [14] *Interconnection for Wind Energy*, FERC Order 661, June 2005.



Lina He (S'11) received her B.S. and M.S. degrees from Huazhong University of Science and Technology, China, in 2007 and 2009, respectively. She is pursuing the Ph.D. degree in electrical engineering at University College Dublin, Ireland. She was an Engineer at Tianjin Electric Power Corporation, State Grid, China during 2009-2010. Her research interests include the protection and defense of HVDC offshore wind network.



Chen-Ching Liu (F'94) received his Ph.D. degree from University of California, Berkeley. He is presently Boeing Distinguished Professor at Washington State University, USA and Professor of Power Systems at University College Dublin, Ireland. He was Palmer Chair Professor of Electrical Engineering at Iowa State University and a Professor of Electrical Engineering at the University of Washington, USA. Dr. Liu received an IEEE Third Millennium Medal in 2000 and the IEEE Power and Energy Society Outstanding Power Engineering Educator Award in 2004. Professor Liu is a Fellow of the IEEE.